



Metal(lod)s Removal Response to the Seasonal Freeze–Thaw Cycle in Semi-passive Pilot Scale Bioreactors

Morgane Desmau¹ · Rachel Simister² · Susan A. Baldwin³ · Guillaume Nielsen¹

Received: 19 December 2023 / Accepted: 16 August 2024 / Published online: 3 September 2024
© The Author(s) 2024, corrected publication 2024

Abstract

There is an increasing demand for cost-effective semi-passive water treatment that can withstand challenging climatic conditions and effectively and sustainably manage mine-impacted water in (sub)arctic regions. This study investigated the ability of four pilot-scale bioreactors inoculated with locally sourced bacteria and affected by a freeze–thaw cycle to remove selenium and antimony. The bioreactors were operated at a Canadian (sub)arctic mine for a year. Two duplicate bioreactors were installed in a heated shed that was maintained at 5 °C over the winter, while two other duplicates were installed outdoors and left to freeze. The removal rate of selenium and antimony was monitored weekly, while a genomic characterization of the microbial populations in the bioreactors was performed monthly. The overall percentage of selenium and antimony removal was similar in the outside (10–93% Se, 20–96% Sb) and inside (35–94% Se, 10–95% Sb) bioreactors, apart from the spring thawing period when removal in the outdoor bioreactors was slightly lower for Se. The dominant taxonomic groups of microbial populations in all bioreactors were Bacteroidota, Firmicutes, Desulfobacterota and Proteobacteria. The microbial population composition was consistent and re-established quickly after spring thaw in the outside bioreactors. This demonstrated that the removal capacity of bioreactors inoculated with locally sourced bacteria was mostly unaffected by a freeze–thaw cycle, highlighting the strength of using local resources to design bioreactors in extreme climatic conditions.

Keywords Sulfate reduction · Mine-contact water · (sub)arctic · Genomics · Bioremediation

Introduction

The (sub)arctic regions are rich in strategic mineral resources and are becoming more accessible thanks to infrastructure development and expanding interest from the mining sector (Haley et al. 2011; Tiainen et al. 2015). However, when not adequately managed, mining activities present environmental concerns (Sengupta 2021). One major challenge is controlling the release of mine-impacted water (MIW) into the environment. Unmanaged MIW containing metal(lod)s and other inorganic constituents at concentrations exceeding the regulated limits can have deleterious effects on downstream

aquatic environments (Leppänen et al. 2017; Wright et al. 2015). Thus, the development of sustainable, efficient, and cost-effective water treatment technologies is required for mineral exploitation to expand in (sub)arctic areas.

Different water treatment technologies are available. Active chemical water treatment technologies are still preferred for operating mines (Qin et al. 2019). These systems rely heavily on infrastructure, labor, and chemical reagent utilization, usually producing large amounts of sludge or liquid waste, which limits their sustainability over the long term (Ness et al. 2014). Passive and semi-passive water treatment systems are considered viable alternatives in closure scenarios because they are more economical and environmentally friendly (Martin et al. 2009). For example, in Canada, many active mines proposed passive or semi-passive treatment technologies for their future closure plans (Eagle Gold mine's closure plan (Victoria Gold Corp. 2022); Casino mine's closure plan (Brodie Consulting Ltd. and Casino Mining Corporation, 2013)). However, local regulation entities such as the Yukon Environmental and

✉ Guillaume Nielsen
gnielsen@yukonu.ca

¹ Yukon University Research Center, 500 College Drive, PO Box 2799, Whitehorse, YT Y1A 5K4, Canada

² 3R Circuits Solutions Inc, 3600 Gilmore Way, Burnaby, BC V5G 4R8, Canada

³ Chemical and Biological Engineering, Univ of British Columbia, 2360 East Mall, Vancouver, BC V6T 1Z3, Canada

Socio-Economic Assessment Board (YESAB) lack scientific evidence to approve these plans.

Passive water treatment technologies mimic natural chemical and biological processes, use natural or residual materials, and need little supervision or maintenance (El Kilani et al. 2021; Johnson and Hallberg 2005; Younger et al. 2002). Semi-passive water treatment technologies are similar to passive water treatment but require some periodic management, such as carbon source addition (Martin et al. 2009). The mining sector has demonstrated a strong interest in bioreactors (BRs) (Habe et al. 2020; Neculita et al. 2007).

BRs are constructed systems that support a biologically active environment able to sustain processes favoring the removal of specific inorganic constituents to reach levels that meet environmentally safe aquatic life standards. BRs are made of reactive mixtures involving an organic carbon source to support bacterial activity, a structural agent for hydraulic parameters, and often an inoculum (Ben Ali et al. 2020). Preferred processes in BRs lead to the precipitation of inorganic contaminants as metal(loid) sulfides as the result of reduction of sulfate to sulfide due to the bacterial activity of sulfate-reducing bacteria (SRB) (Neculita et al. 2007). However, precipitation, sorption, ion exchange, and complexation mechanisms have also been observed in BRs, specifically for neutral ($6 < \text{pH} < 9$) MIW (El Kilani et al. 2021). BRs have been used efficiently in the last 30 years for the treatment of both acid ($\text{pH} < 6$) and neutral MIW at the bench and pilot scale, at closed and abandoned sites, but mostly in temperate and semi-arid climates (Ben Ali et al. 2019; Clyde et al. 2016; Genty et al. 2018; Habe et al. 2020; Neculita et al. 2007; Sánchez-Andrea et al. 2014).

The application of BRs in (sub)arctic regions is challenged by the cold climatic and limited resources. Climatic conditions in (sub)arctic regions, specifically in northern America, are characterized by freeze–thaw cycles: long, cold, and dry winters, with temperatures below freezing measured from late September to early June, followed by summer periods characterized by an increase in temperature and long daylight exposure. These patterns lead to multiple freezing and thawing events during the fall and the freshet, while ditches and watercourses that collect MIW often freeze during winter.

Previous studies at low temperatures (10 °C or less) have demonstrated the ability of BRs to successfully and consistently remove contaminants over long periods of time and for both acidic and neutral MIW. Using a heated shed to prevent BRs from freezing, Nielsen et al. (2018a) removed $\approx 90\%$ of zinc and cadmium from neutral MIW during summer (temperature > 15 °C) while during winter, removal decreased to 20–40% (temperature = 5 °C). Similarly, Harrington et al. (2015) observed reductions of 80% in arsenic, antimony, and nickel loads at the semi-buried pilot-scale bioreactor of the Keno Hill Silver District (Yukon, Canada), over one

year and for MIW temperatures between 1 and 10 °C. At the Standard Mine Superfund Site (Colorado, USA), a four-year pilot-scale BR study achieved more than 98% removal of cadmium, copper, zinc, and lead from acidic MIW under alpine climatic conditions (Reisman et al. 2009; Rutkowski 2013). Under (sub)arctic conditions, El Kilani and collaborators observed the absence of SRB growth in their BRs, despite good removal rates due to sorption and precipitation for iron and copper (> 95%) (El Kilani et al. 2021). Nonetheless, nickel removal decreased from $\approx 95\%$ at the beginning to 50–80% at the end of their experiment, due to the absence of SRB, highlighting the importance of these microorganisms for the effective and reliable operation of BRs. Low temperatures restrained bacterial activity by slowing down their metabolic activities (Price and Sowers 2004). SRB are known to be active over a wide range of temperatures between 0 and 80 °C (Odom and Singleton 1993) and metabolically active SRBs have been observed in arctic environments (< 5 °C) (Robador et al. 2009). Nonetheless, passive and semi-passive water treatments are generally challenging in cold climates and previous studies indicate that one of the main challenges faced by the utilization of BRs in the (sub) arctic area is to maintain active bacterial activity (Ben Ali et al. 2019). It also needs to be considered that operation of BRs during the winter in arctic or sub-arctic climates is often impeded due to freezing of the source MIW (for groundwater that does not stay in the 0.5–5 °C range). One question that has not been addressed sufficiently in the literature is how quickly the microbial community can re-establish itself during the thaw and how this subsequently affects BR treatment performance. This is the research question addressed in this study.

To overcome limitations imposed by low or freezing temperatures, previous studies have recommended utilizing: (i) cold-adapted microorganisms in the inoculum or local bacteria inoculum (Zaluski et al. 2003), (ii) installing the biological components at depths below the freezing point of the soil and insulating the BRs with soil or manufactured covers (Gallagher et al. 2012; Reisman et al. 2009), and (iii) supporting bacterial growth and activity by providing an additional carbon source (Nielsen et al. 2018b), transforming passive BRs into semi-passive BRs. The option to use buried or semi-buried BRs has shown promising results in limiting the freezing of the BRs and decontaminating mine-impacted groundwater (Harrington et al. 2015; Reisman et al. 2009). However, treatment of surface MIW is challenging due to resource limitations (insulation materials, soils, etc.) in the North, and the extremely negative temperatures experienced in these (sub)arctic regions (-40 °C), leading to freezing of even semi-buried BRs at mine sites (private communication), which limits their widespread utilization. In addition, and to the best of our knowledge, no study has investigated the effect of freeze–thaw cycles on the operation of BRs at

the pilot scale, as well as the effect of freeze–thaw cycles on the microbial population composition of the BRs and how this might affect removal efficiency.

Se and Sb are two contaminants often found in MIW (Lum et al. 2023; Yan et al. 2022). They are present in MIW either as by-products of mining other metals such as gold or are exploited for their industrial uses. While Se is a nutrient at low concentration, Sb has no known biological role. Several active physicochemical treatment methods exist for Se and Sb but they are usually expensive and produce large amounts of sludge (Laroche et al. 2023; Sinharoy and Lens 2020). For both elements, BRs are considered sustainable, cost-effective, and efficient water treatment technologies in temperate climates (Ramírez-Patiño et al. 2023; Sinharoy and Lens 2020). Over 75% of Se was removed from neutral MIW at the laboratory scale using sulfidogenic BRs (Luo et al. 2008), while Sb in neutral MIW was removed up to 60% in similar BRs (Ramírez-Patiño et al. 2023). In MIW, Se is usually present as oxyanions, either selenite (Se(IV)) or selenate (Se(VI)), depending on the pH and redox state (Sinharoy and Lens 2020). The main mechanism for Se oxyanion removal in BRs is the anaerobic reduction of selenate to selenite to insoluble elemental Se particles through bacterial activity (Yan et al. 2022). Sb can be present as Sb(V) or Sb(III) in MIW at neutral pH (Ramírez-Patiño et al. 2023). Sb reduction in BRs occurs through either intracellular pathways (methylation) or extracellular pathways. Extracellular pathways include the dissimilatory pathway, with Sb(V) used as an electron acceptor and the sulfate reduction pathway with chemical reduction of Sb(V) to Sb(III) by the H₂S produced by SRB during the sulfate-reducing process. In addition, the presence of biogenic sulfide favors the precipitation of metal(loid)s sulfide (Ramírez-Patiño et al. 2023).

Here, we investigated the ability of semi-passive BRs, inoculated with locally sourced bacterial populations, to remove selenium (Se) and antimony (Sb) from MIW, under (sub)arctic conditions on-site (i.e. exposed to a natural freeze–thaw cycle). The goals of the present study were to investigate: (i) the ability of a native inoculum to develop an efficient and stable SRB community in BRs subject to freeze and thaw cycles and (ii) the performance of BRs that were inactive over winter (freeze) in comparison with the performance of BRs that did not freeze over winter.

Materials and Methods

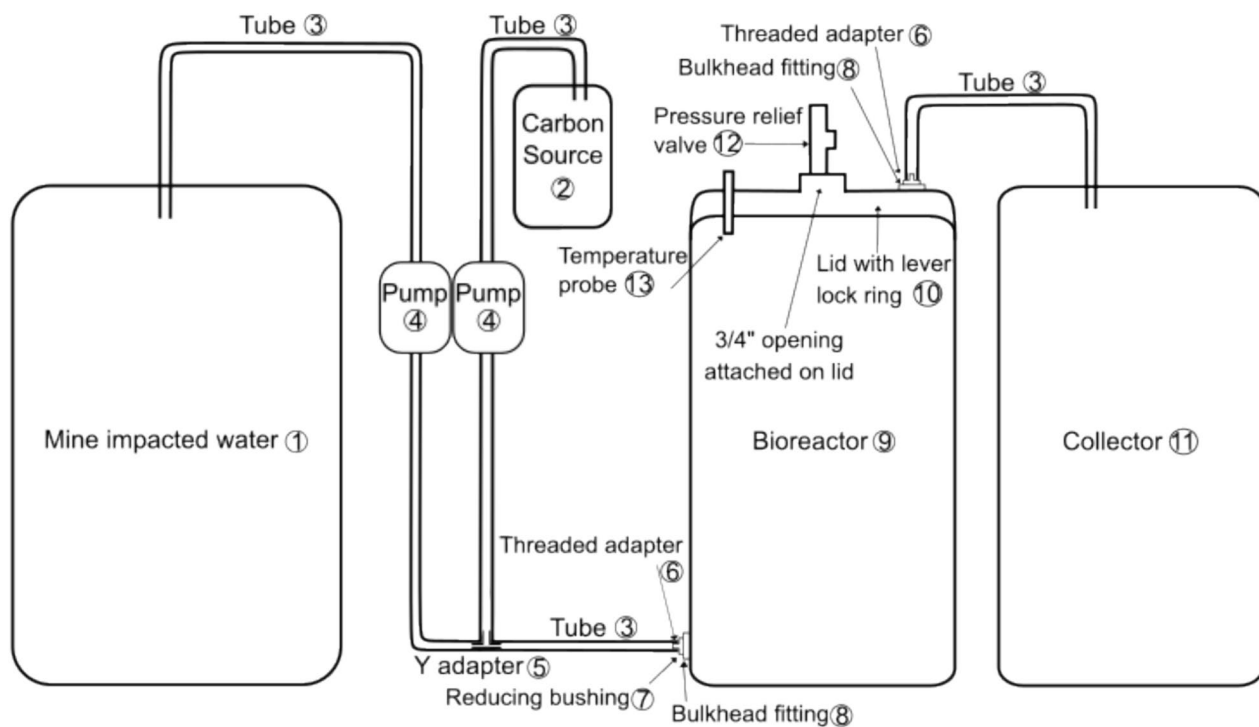
Experimental Setup

Four pilot-scale BRs were installed at the remote operating Eagle Gold Mine located in central Yukon Territory, Canada. Each BR vessel was an open-top 208 L polyethylene drum covered with a lid and a steel lever lock (Uline, Milton,

Canada). Duplicate BRs (BR1a and BR1b) were placed in a shed that was heated to maintain a minimum temperature of 5 °C over the winter and left to fluctuate with outside temperature when over 5 °C. Duplicates BR2a and BR2b were installed outside of the shed where they were exposed to freezing temperatures. MIW was fed into all BRs from the same feed tank that was situated inside the shed. MIW and the carbon source, a molasses solution contained in a 10 L glass jar, were fed into the BRs through inlet pipes installed near the bottom of each vessel. The MIW flowed from the bottom to the top of the BR vessels to ensure anoxic conditions. Oxidation–reduction potential (ORP) was measured monthly from a location approximately halfway up the vessel in all BRs to check and confirm reducing conditions. The outflow from the top of each BR went to its own collector drum. The two collector drums inside of the shed remained open, while the other two collector drums outside of the shed were covered with lids and steel lever locks to prevent particles from entering the vessels. Temperatures inside the BRs were monitored using Oakton Temperature Probes 5+ installed at the top of the BRs, reaching the inside through a hole drilled in the BRs' lid and sealed with silicone to prevent air ingress. Apollo pressure relief valves were also installed on the lid to prevent the pressure exceeding 0.21 MPa (30 psi) in the BRs (Fig. 1).

Each BR was filled with 20% v/v locally sourced, shredded spruce wood chips 2.5–5 cm in size and 20% v/v inoculum. Wood chips were added as a support structure material for bacterial growth. The inoculum was a mixture of sediment samples from two different wetlands in the same Eagle Gold Mine drainage, at locations 0459110E 7100937N and 0458249E 7099695N, respectively. The wood chips and inoculum were mixed thoroughly in the BRs and filled the vessels to a depth of ≈ 60 cm. MIW (≈ 170 L) was added to cover the reactive material and fill the vessel to the brim. This was done to ensure anaerobic conditions inside the reactive material. A passive sampling method was used to collect the microorganisms growing inside the BRs. The microorganisms sampled were assumed to be representative of the bacterial communities within the BRs, originating from either the inoculum or the MIW entering the BRs. Sampling bags were made with light cotton material and filled with the same sediment used to inoculate the BRs. Twelve sampling bags (one for each monthly sample) were suspended in the middle of each BR, with fishing lines fed through a hole in each BR lid at the beginning of the experiment. The hole was then sealed with silicon to prevent air ingress into the BRs.

The MIW used to feed the BRs was restocked on a weekly basis from two different sources at Eagle Gold Mine, referred to as source 1 and source 2. From September 7 to November 15, 2019, and from May 12 to September 27, 2020, MIW was collected from source 1: Ditch A which



Number	Name	Number	Name	Number	Name
①	Intermediate bulk container	⑥	1/8" NPT - 1/8" ID nylon threaded adapter	⑪	55 gallon open head polyethylene drum
②	10L glass with magnetic stirrer	⑦	3/4" NPT - 1/8" ID nylon reducing bushing	⑫	30-psi pressure relief valve
③	Masterflex L/S 16 Tubing	⑧	2" NPT - 3/4" NPT nylon bulkhead fitting	⑬	Digi-sense replacement temperature probe
④	Masterflex peristaltic pump	⑨	55 gallon open head polyethylene drum		
⑤	1/8" ID Y adapter	⑩	Polyethylene lid with steel lever lock ring		

Fig. 1 Experimental setup. The same MIW feed tank fed all four bioreactors, those outside and inside the shed

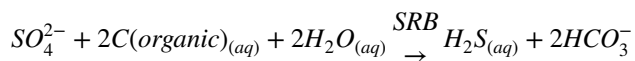
collects drainage from one of the waste rock piles at Eagle Gold mine, the Platinum Gulch Waste Rock Storage Area. Between those periods, when Ditch A was not accessible due to freezing, MIW was collected from source 2: a collection pond used to store MIW from Ditch A that does not freeze all the way to the bottom during winter.

Operation and Experimental Design

The BRs were operated with an expected two-week hydraulic retention time (HRT) based on a previous study with similar MIW parameters and carbon sources (Nielsen et al. 2018a). The MIW flow rate, controlled by peristaltic pumps (Cole Palmer Masterflex L/S Standard Digital Drives), was 10.6 mL/min giving an average HRT of 11 days over the year.

The carbon source used in this study was molasses (Crosby's 100% Natural Fancy Molasses). This carbon source was used successfully in previous studies to support the growth of SRB (Muyzer and Stams 2008; Nielsen et al. 2018a). In addition, molasses supports a diverse bacterial community

including species other than SRB (Zhao et al. 2010), resulting in greater resilience of the bacterial community in the BRs to environmental perturbations (Allison and Martiny 2008; Ayala-Muñoz et al. 2021). The molasses solution was prepared biweekly. The amount of molasses added was based on the stoichiometric requirement (Eq. 1). Considering a maximum sulfate concentration in the MIW feed of 100 mg/L, the molasses concentration was fed into the BRs at 25 mg-C/L. Molasses solutions were pumped into the BRs for 22 min/day at a flow rate of 6 mL/min to achieve the targeted calculated total organic carbon (TOC) concentration per day.



Given the site's remoteness and the climatic conditions during winter, treated water coming out of each BR was collected weekly from the effluent drums after mixing by stirring, giving bulk accumulated effluent samples, also referred to as "effluent samples". The total volume of effluent collected in each drum over the previous week was recorded

to verify accurate pumping rates and HRTs. Effluent drums were emptied after each weekly sampling event. The electrical EC (EC) and pH of the MIW and effluents were recorded weekly using an Oakton PCD650m pH meter equipped with a double junction Cole Palmer Ag/AgCl electrode. Samples for TOC were preserved with sulfuric acid (2%, v/v). Samples for metals and metalloids were preserved with nitric acid (2%, v/v). Every month, one passive microbiological sample bag was removed from each BR. Sampling bags were frozen by liquid nitrogen in a thermo-flask (Thermo Fisher Scientific container 2122) immediately after collection and transported from the field to the laboratory for storage at -86°C until DNA extraction. Liquid samples were analyzed by ALS, Burnaby, for metals and metalloids (EPA 200/6020A) and TOC (APHA 5310B). Sulfate analysis was performed following the protocol described by Nielsen and collaborators (Nielsen et al. 2018a). Uncertainties were estimated based on the analysis uncertainties (duplicate). To estimate the removal efficiencies (RE) for the sulfate, Se, Sb, and carbon, the following was used: $RE = [(In-Out)/In] \times 100$). For an effluent (out) at week N, the concentration measured in the influent (In) at week N-2 was used, to fit the closest with the HRT.

DNA Extraction, Sequencing, and Bioinformatics

Genomic DNA was extracted from 0.25 g subsamples taken from homogenized passive sample bag contents using the DNeasy PowerSoil Pro Kit (QIAGEN) following the manufacturer's instructions. DNA concentrations were measured using an Invitrogen™ Qubit™ 3.0 Fluorometer (Thermo Fisher Scientific). The purity of the extracted DNA was measured using a NanoDrop ND-2000 ultraviolet-visible spectrophotometer (NanoDrop Technologies) at 260 nm for nucleic acid. To ensure the purity of the extracted DNA, absorbance was also measured at 230 nm for organic contamination and 280 nm for protein contamination. For pure DNA samples, absorbance ratios should be A260/A280 1.8–2.0 and A260/A230 2.0 (Armbrecht 2013). If the DNA did not pass quality control, it was purified using the DNeasy PowerClean Pro Cleanup kit (QIAGEN).

The 16S rRNA variable region V4 to V5 was amplified using primers 515F-Y and 926R (Parada et al. 2016; Walters et al. 2016) and sequenced on an Illumina MiSeq in the Biofactorial Core Facility in the Life Sciences Institute of the University of British Columbia. The raw sequence data were converted into amplicon sequence variants (ASV) by applying the open-source software package DADA2 (Callahan et al. 2016) for modelling and correcting illumina-sequenced amplicon errors, using the Qiime2 suite of tools (Bolyen et al. 2019). A frequency table with relative abundance information for each ASV was produced. The taxonomic classification of each ASV was assigned by aligning

the representative sequence to the Silva SSU database (version 138.1) (Warnow 2015). All data were visualized in R or Excel. For a- and b-diversity measures, all samples were subsampled to the lowest coverage depth, and standard indices were calculated in Qiime2. Raw sequencing data are available under NCBI BioProject ID PRJNA924841.

Carbon Leaching Experiments

Wood chips were chosen as the reactive material to support bacterial growth in the BRs for its availability in the (sub)arctic and at the mine site. However, wood chips have the potential to leach TOC and impact bacterial growth. To assess the TOC leaching potential of the wood chips used in the BRs, two duplicate 2 L columns filled with 20% v/v wood chips (equivalent to 72 g of wood chips per column) were installed in the laboratory at room temperature. DI water was pumped from the bottom to the top of the columns by a peristaltic pump (Cole Palmer Masterflex L/S Standard Digital Drives) for 35 days. The pump was set at 0.08 RPM to achieve an HRT of 14 days, similar to the one used in the pilot scale BRs. Weekly batches of leachate effluent were collected in 2 L jars. Homogenized samples were preserved with sulfuric acid (2% v/v) and sent to ALS, Burnaby, for TOC analysis.

Results

Operating Conditions

All of the BRs were operated from Sept. 7, 2019, to Sept. 27, 2020. Between Oct. 16 and 25, 2019, the temperature outside of the shed started to fall below freezing during the day (supplemental Fig. S-1), indicating most likely even colder temperatures overnight. On Oct. 15, before BR2a froze completely, the last passive microbiological sample bag was collected in BR2a after breaking the ice partially forming in the BRs. At this time, BR2b was already completely frozen and it was impossible to collect a bag. From the end of October 2019 to May 12, 2020, the temperature outside the shed was below 0 °C, and MIW couldn't flow through BR2a and BR2b until May 19, 2020, due to the freezing of BR2a and BR2b. During the few weeks before the complete freezing of the BRs and the complete thawing of the BRs, a succession of small freeze–thaw cycles likely occurred that was unfortunately not recorded given the weekly sampling. Throughout this paper, the period from mid-October 2019 to mid-May 2020, is referred to as the “winter” period, during which BR2a and BR2b were either fully or partially frozen and no MIW was flowing through them. BR1s (BR1a and BR1b), located inside the shed, were prevented from freezing and continued to operate throughout winter. Thawing took place

during May and June 2020 (“spring”), during which the flow of MIW through BR2a and BR2b recommenced. The “summer” period included July and August 2020, and the “fall” was September 2020.

The pH of the MIW feed varied from 7.2 to 8.5 throughout the experiment, with an average of 8.0 ± 0.4 , with one outlier event measured at 9.3 (supplemental Fig. S-2). The pHs measured in the BRs were circumneutral for the duration of their operating periods: the pH of BR1a averaged at 7.5 ± 0.4 , BR1b averaged 7.6 ± 0.4 , BR2a averaged 7.1 ± 0.3 , and BR2b averaged 7.0 ± 0.4 . The EC measurements were used to estimate the concentration of total dissolved solids (supplemental Fig. S-3). The MIW in the winter months had a higher EC ($583 \pm 47 \mu\text{S}/\text{cm}$) than that used during the rest of the year ($232 \pm 92 \mu\text{S}/\text{cm}$). The change of source in mid-November did not strongly affect the EC of the MIW. From September to November 2019, source 1 had an EC of $406 \pm 163 \mu\text{S}/\text{cm}$ while source 2 had an average EC of $562 \pm 130 \mu\text{S}/\text{cm}$ (December 2019 to May 2020). In addition, as shown in supplemental Fig. S-3, the EC of the MIW in the last sampling of source 1 in November 2019 was $614 \mu\text{S}/\text{cm}$ and the first sampling of source 2 was $625 \mu\text{S}/\text{cm}$, indicating similar EC between the two MIW sources at a given time. The difference in EC between the winter months and the rest of the year was thus independent of the source modification. The MIW EC trends indicate an important parameter affecting semi-passive treatment design: the natural seasonal concentration dilution effect. During the freshet from May to July, with snow melt and high-water flows, a dilution effect was observed with lower ECs of $\approx 300 \mu\text{S}/\text{cm}$. On the other hand, during the winter months, from October to April, a concentration effect was observed with MIW EC increasing to $\approx 650 \mu\text{S}/\text{cm}$. These natural fluctuations affect the initial concentrations of the contaminants of concern and subsequently the removal percentages. The major cation in the MIW was Ca^{2+} , with concentrations ranging from 22 to 90 mg/L. The EC and Ca^{2+} concentration in the BR effluents tracked that of the MIW (supplemental Figs. S-3 and S-4).

The temperatures in BR1a and BR1b varied from highs of 24.7°C on Oct. 11, 2019, and 22.3°C on Nov. 15, 2019, to lows of 3.7 and 2.9°C on April 22, 2020, respectively (Fig. S-1). The highest temperatures for BR2a and BR2b were recorded on Oct. 11, 2019, at 20.2°C and June 16, 2020, at 19.2°C , respectively. BR1a, BR1b, BR2a, and BR2b operated at average temperatures of 12 ± 3 , 13 ± 3 , 11 ± 3 , $13 \pm 4^\circ\text{C}$, respectively, from mid-May 2020 to the end of September 2020. The monthly ORP measurements (supplemental Table S-1) ranged between -112.7 to -438.2 mV for BR1a, -85.7 to -307.3 mV for BR1b, -113.7 to -281.9 mV for BR2a, and -108.4 to -298.3 mV for BR2b. The most reducing conditions were reached at different times over the year for the four BRs, with the least reducing conditions measured during the first

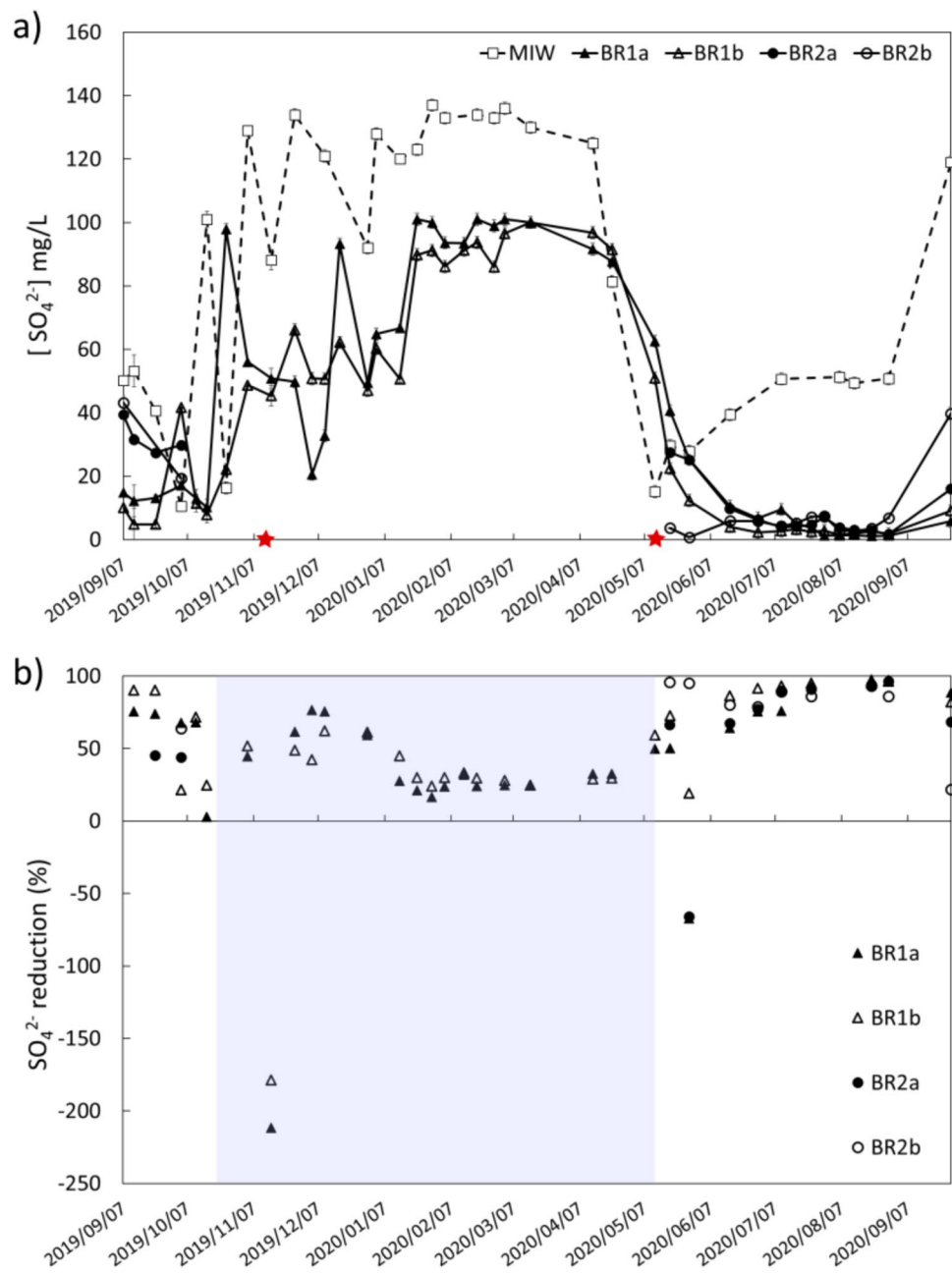
month of operation (September 2019) for BR1a, BR2a, and BR2b, and in December 2019 for BR1b.

Sulfate Reduction

The sulfate concentrations in the MIW feed varied over the year between a low of $10.5 \pm 0.5 \text{ mg/L}$ on Oct. 4, 2019, and a high of $137.0 \pm 2.6 \text{ mg/L}$ on January 29, 2020 (Fig. 2a). Until Oct. 11, 2019, and after April 22, 2020, the concentration of sulfate in the MIW was $< 60 \text{ mg/L}$. The change from source 1 to source 2 occurred on Nov. 11, 2019, and source 2 was used until May 12, 2020. The sulfate concentration in source 1 was $129.0 \pm 0.5 \text{ mg/L}$ during the last sampling on Nov. 4, 2019, and $88.2 \pm 3.2 \text{ mg/L}$ for the first sampling in source 2 on Nov. 15, 2019. Over winter, the sulfate concentration in the MIW was on average higher ($115 \pm 17 \text{ mg/L}$) than during fall 2019 ($39 \pm 17 \text{ mg/L}$), spring ($28 \pm 9 \text{ mg/L}$), and summer 2020 ($51 \pm 1 \text{ mg/L}$). Thus, the increase in sulfate concentration cannot be attributed to the change in the MIW source. From mid-October 2019 to mid-January 2020, the sulfate concentration increased gradually in a semi-oscillatory fashion with a periodicity of about two weeks, which could correspond to the refilling of the feed tank.

Sulfate concentration trends in the bioreactor (BR) effluents followed those in the MIW, with higher concentrations during the winter months than during the spring, summer, and fall (Fig. 2a). Prior to winter, BR2a and BR2b effluent sulfate concentrations (32 ± 5 and $31 \pm 12 \text{ mg/L}$, respectively) were higher than those in the BR1 effluents (14 ± 2 and $15 \pm 13 \text{ mg/L}$, respectively). However, after the spring thaw and throughout the summer and fall of 2020, both the indoor and outdoor bioreactor pairs achieved similar sulfate concentrations in their effluents (around 5 mg/L). Percentages of sulfate reduction efficiency (Reduction Efficiency = $[(\text{In}-\text{Out})/\text{In}] \times 100$) were positive in all BRs over the entire experiment, except in two instances for BR1a and one instance in BR1b and BR2a (Fig. 2b). The negative reduction efficiencies were due to the low sulfate concentrations measured in the MIW. In addition, two of them were observed during the thaw, a period with changes in temperature and freezing conditions for the outside BRs. Overall, BR1a and BR1b presented similar behavior in terms of sulfate reduction except before winter, due to the equilibration of the BRs, and in May 2020 (spring), because of the important variation in temperature during the day (Fig. S-1), and likely between days and nights inside the shed. During winter, sulfate reduction efficiencies were between 17 and 76% for BR1a and 24% and 62% for BR1b. In both cases, the higher reduction efficiency values were measured at the beginning of winter and were followed by a decrease, with values stabilizing around 30% until spring. From July 2020 until the end of the study, the sulfate reduction efficiency in BR1a and BR1b remained high ($> 75\%$).

Fig. 2 Evolution of sulfate concentration (mg/L) (a) and percentage of sulfate reduction (b) in mine impacted water (MIW, empty square, and dashed line), BR1a (black triangle and full line), BR1b (empty triangle and full line), BR2a (black circle and full line) and BR2b (empty circle and full line) function of time. The red stars in (a) correspond to the change in the MIW source (from source 1 to source 2, and then from source 2 to source 1). The period during which BR2a and BR2b were considered frozen is represented in blue in (b)



Before winter, $\approx 45\%$ of the sulfate was reduced in BR2a, and 64% in BR2b. During the May thaw, sulfate reduction was important in BR2b ($> 95\%$), while in BR2a an important variation was observed (from -60% to $+60\%$), indicating different behaviors between the two outside BRs, likely due to the thawing. From July 2020 to the end of the study, the percentage of sulfate reduction remained high ($> 75\%$) in BR2a and BR2b, similar to what was observed in BR1a and BR1b, except for the last data point. For BR2a and BR2b, sulfate reduction efficiencies dropped to 68% and 22% , respectively, at the end of September 2020. While temperatures above 10°C were measured at the end of September

2020 (Fig. S-1), from the end of August to mid-September, the temperatures were closer to 0°C , which could have slowed down sulfate reduction in the outside BRs.

Carbon Source Consumption

To supply enough carbon (C) for the reduction of the sulfate entering the BRs, the TOC was measured in the MIW feed and supplemental C was added through a molasses solution (2 mg/L) to reach the targeted amount of TOC, according to Eq. 1. Fig. S-5a presents the calculated TOC concentration

obtained by adding the initial TOC in MIW and the TOC added through the molasses solution.

From September to December 2019, the percentage of TOC removal varied in all of the BRs (Fig. S-5), with negative values observed for BR1a, BR1b, and BR2b, which indicated the release of carbon from a source inside the BRs. After December and until the end of the experiment, TOC removal in BR1a and BR1b stabilized in the positive, with an average carbon consumption of $51 \pm 23\%$ for BR1a and $61 \pm 6\%$ for BR1b. When sampling of BR2s restarted during the spring and until the end of the experiment, TOC removal alternated negative and positive removal percentages (Figs. S-5b). This alternation was likely due to equilibration in the bacterial population and bacterial activities (Fig. 5) after the restart of the BRs.

Laboratory leaching experiments were performed to estimate the spruce wood chips' leaching capabilities. Spruce wood chips leached 2.1 mg-C/g-wood-chips in column 1 and 1.5 mg-C/g-wood-chips in column 2 over the first week of their operation (Fig. S-6). After 5 weeks, the TOC leached from the spruce wood chips decreased to 0.6 mg-C/g-wood-chips in column 1 and 0.5 mg-C/g-wood-chips in column 2 (Fig. S-6). The total amount of carbon leached from columns 1 and 2 were 6.5 and 5.0 mg-C/g-wood chips (dry weight), respectively, over the five weeks of experiments.

Metal(loid)s

Iron Leaching

Iron (Fe) concentrations in the MIW were less than 1.5 mg/L, except for eight peak events, with one reaching 35.2 ± 1.1 mg/L (supplemental Fig. S-7). For the most part, the Fe concentrations were higher in the effluents than in the MIW, which indicates that Fe was being released from the BRs. The main source of Fe in the BRs was likely the inoculum. Wetlands are known to accumulate Fe (Doyle and Otte 1997) and sediments used as inoculum were taken from a wetland close to the mine site. Further characterization of the inoculum would be needed to validate this hypothesis.

Antimony

The Sb concentrations in the MIW were between 0.5 ± 0.0 and 5.1 ± 0.2 µg/L during most of the study period (Fig. 3a). Two events with higher Sb concentrations (10.9 ± 0.4 and 12.5 ± 0.5 µg/L) were detected in April and August 2020, respectively. The Sb concentration during the last sampling event of source 1 in November 2019 (3.2 ± 0.1 µg/L) was similar to the first sampling event of source 2 in November 2019 (3.6 ± 0.1 µg/L). In May, the difference between the two sources was more important: 7.7 ± 0.3 µg/L for the last sampling with source 2 vs. 2.3 ± 0.1 for the first sampling

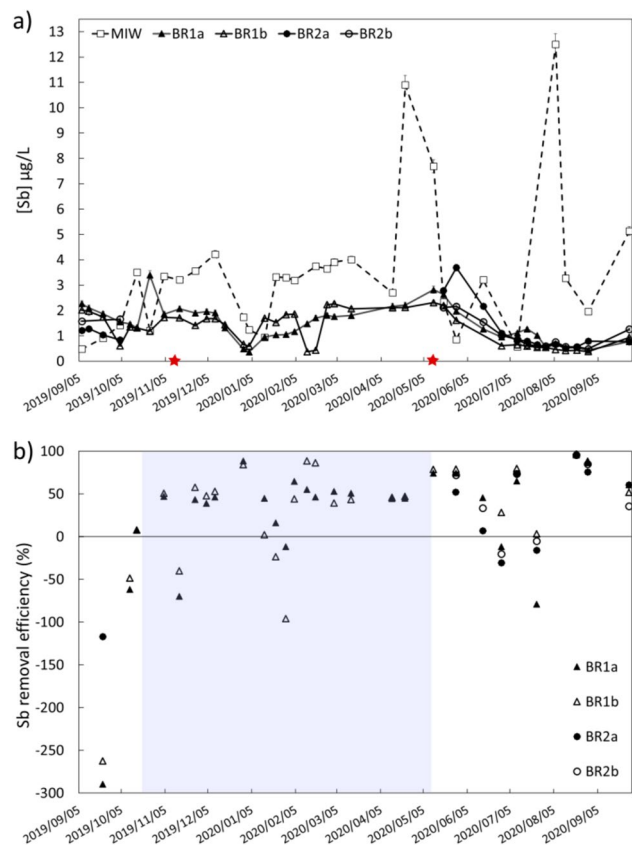


Fig. 3 Evolution of antimony concentration (mg/L) (a) and percentage of antimony removal efficiency (b) in mine impacted water (MIW, empty square, and dashed line), BR1a (black triangle and full line), BR1b (empty triangle and full line), BR2a (black circle and full line) and BR2b (empty circle and full line) function of time. The red stars in (a) correspond to the change in the MIW source (from source 1 to source 2, and then from source 2 to source 1). The period during which BR2a and BR2b were considered frozen is represented in blue in (b)

in source 1. However, as mentioned previously, they were even higher in August when the MIW source 1 was sampled.

The Sb concentration trends over time were similar in the effluents of the four BRs, with lower concentrations than those of the MIW. The Sb concentrations in the effluents ranged between $0.4\text{--}2.8$, $0.4\text{--}2.3$, $0.5\text{--}3.7$, and $0.5\text{--}2.2$ µg/L in BR1a, BR1b, BR2a, and BR2b, respectively, over the year.

The Sb removal efficiency in BR1a and BR1b was positive most of the time, with the highest removal of 96% for both BRs, reached on August 21, 2020 (Fig. 3b). On the same date, the maximum RE were also reached for BR2a and BR2b (96% for both BRs). Negative Sb RE was observed on seven instances for BR1a, five for BR1b, three for BR2a, and two for BR2b. BR2a and BR2b had fewer negative Sb reduction efficiency events because of the sparser amount of data for the outside BRs. The most negative Sb reduction

efficiency values were measured at the beginning of the experiment, most likely due to the BRs start-up. Interestingly, all the negative Sb reduction efficiency were observed on the same date. When BR1a presented negative reduction efficiency but BR1b did not, the Sb reduction efficiency for BR1b were below 30%. For all negative Sb reduction efficiency values or Sb reduction efficiency values < 30%, the Sb concentration in the MIW was below 1.5 µg/L. The percentage of Sb reduction efficiency also tended to present values closer to 40–50% when the concentrations in Sb in MIW were between 1.5 and 3 µg/L. This could indicate that the inside and outside BRs all saw their ability to remove Sb decreased when Sb concentrations dropped below 3 µg/L. Despite the negative or low Sb reduction efficiency, the Sb concentrations in the BRs' effluents were still below 1.5 µg/L, i.e. below the limit for Sb in drinkable water of 6 µg/L in Canada (Health Canada/Santé Canada 2024).

Selenium

Over the year, the Se in the MIW varied in concentration between 0.1 and 1.7 µg/L (Fig. 4a), with a tendency to be above 0.6 µg/L during spring and summer. As for Sb and sulfate, the Se concentration did not vary in the MIW when the source changed. In November, the last sampling event with source 1 had a Se concentration of 0.3 µg/L while the Se concentration for the first sampling event with source 2 was 0.3 µg/L. In May, the difference was more important (1.7 µg/L for source 2 vs. 0.7 µg/L for source 1). However, the Se concentration detected in source 1 (0.7 µg/L) was similar to the concentration detected in source 2 between November and May (0.1–0.8 µg/L).

Overall, Se concentrations in BR1a and BR1b effluent were below those in the MIW, except for the first month of operation, and remained between 0.05 and 0.7 µg/L (Fig. 4a). Se removal in BR2a and BR2b was similar to that observed in BR1s, except after the spring thaw when BR2a and BR2b Se concentrations were closer or above 0.5 µg/L, while in BR1s they were below 0.2 µg/L.

The Se removal efficiencies in BR1a and BR1b were between 4–93% and 0.5–94%, respectively (Fig. 4b). During its operating periods, BR2a and BR2b achieved similar extents of Se removal, with the highest removals of 94% and 89%, respectively. During the thaw (May 2020), BR2a and BR2b Se removal efficiencies were lower (60 and 78%, respectively) compared to BR1a and BR1b during the same period (87 and 92%, respectively). Negative or low (< 10%) Se removal efficiencies were measured during winter (from November 2019 to January 2020) in BR1a and BR1b. There were no specific trends between MIW concentration and lowest removal efficiency values. As it occurred in the first part of winter, it could be linked to an adaptation of bacterial activities to the decrease in temperature in the BRs.

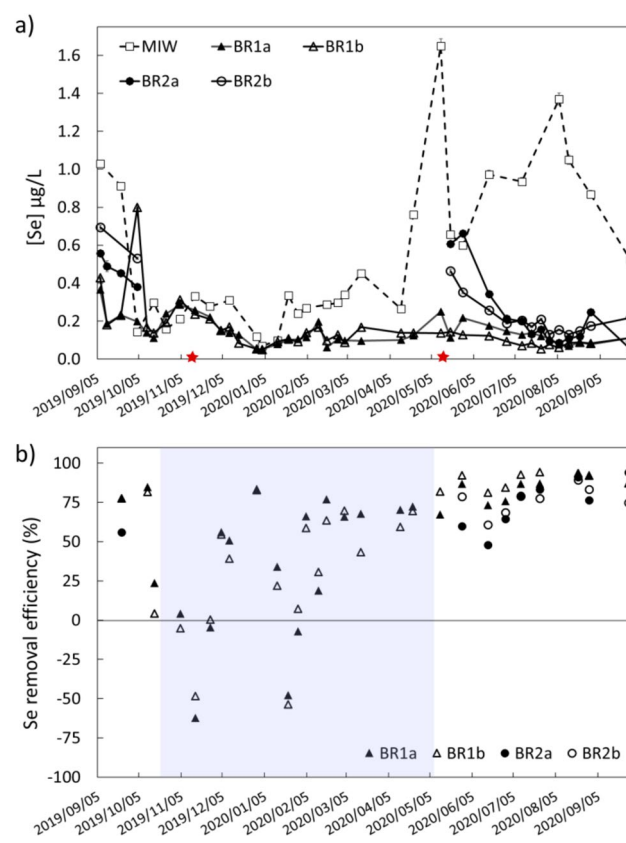


Fig. 4 Evolution of selenium concentration (mg/L) (a) and percentage of antimony removal efficiency (b) in mine impacted water (MIW, empty square, and dashed line), BR1a (black triangle and full line), BR1b (empty triangle and full line), BR2a (black circle and full line) and BR2b (empty circle and full line) function of time. The red stars in (a) correspond to the change in the MIW source (from source 1 to source 2, and then from source 2 to source 1). The period during which BR2a and BR2b were considered frozen is represented in blue in (b)

Bacterial Population Shifts

Overall Microbial Population Composition and Trends at a High Taxonomic Level: Phylum

For all BRs and consistently throughout the study period, the microbial population was constrained to 11 dominant phyla (Fig. 5), the most abundant being the Bacteroidota, Firmicutes, Desulfobacterota and Proteobacteria. Many members of the Desulfobacterota are known to perform sulfate reduction and this phylum was represented at the highest relative abundance in the indoor BRs (BR1a and b) during winter. They were at their lowest relative abundance in these same BRs the following summer. Overall, the prevalence of Desulfobacterota was lower post-spring 2020 in all BRs than previously. Desulfobacterota were more dominant in BR2 than BR1 post-spring 2020, but their percentage relative abundance varied to a greater degree in BR2 than in BR1.

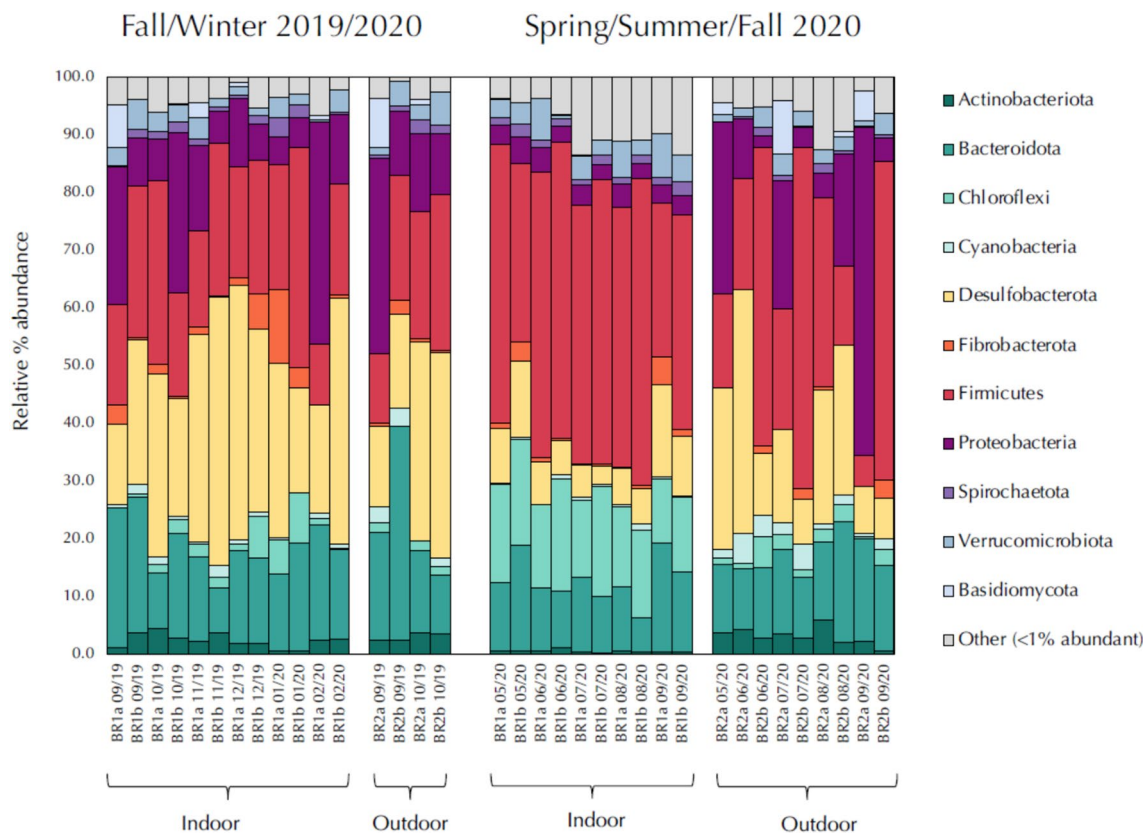


Fig. 5 Side-by-side comparison by seasons of the indoor and outdoor BRs' microbial populations at the phylum level. The category “Other” refers to the sum of all rare ASVs that were present each at less than 1% of the total population

Firmicutes were dominant throughout most BRs and seasons. These heterotrophic microorganisms are involved in the breakdown of complex carbon compounds through hydrolysis and fermentation. These might include compounds in the molasses fed to the BRs, dissolved organic carbon entering with the MIW feed, products from decomposing wood chips or carbon released from dead biomass (Liu et al. 2018; Sharmin et al. 2013). The Bacteroidota phylum had members known to be heterotrophic microorganisms, often known for scavenging partially degraded organic compounds (Mei et al. 2020a). Members of this group were present throughout the operation of the BRs.

It is known that SRB, Firmicutes, and Bacteroidota form syntrophic communities that cycle carbon. Sulfate-reducing bacteria and other Desulfobacterota and Proteobacteria benefit from the degradation products produced by Firmicutes and Bacteroidota. It was observed in other studies of MIW treatment by BRs that the relative abundance of fermenters and SRB vary cyclically out of phase with each other due to carbon cycling (Baldwin et al. 2016).

In a few instances, Proteobacteria were dominant, such as in BR2a during Fall 2019 and Fall 2020. These are functionally versatile microorganisms, some of which are

involved in nitrogen cycling and/or oxidation-reduction of metals, which are important processes in BRs treating MIW (Johnson et al. 2019). The compositional differences between the indoor and outdoor BRs are not easily discernible at the phylum taxonomic level.

Variability in the bacterial population composition between the duplicate indoor and outdoor reactors was observed (Fig. 5). BR2a had a higher relative abundance of Desulfobacterota than BR2b. BR2b had compositionally more Firmicutes than Proteobacteria, whereas BR2a Proteobacteria were more prevalent. Bacterial population composition at the phylum level varied between the BR1 replicates during Fall 2019 and Winter; however, after the thaw, from Spring 2020 onwards, the microbial population composition in the two indoor BRs was more consistent.

Comparing changes in the population composition over the seasons (Fig. 5), the Desulfobacterota were much less dominant in the indoor BRs post-spring 2020 than in fall 2019/winter 2020. The overall population composition in the indoor BRs was consistent over time from spring 2020 onwards, whereas the population composition varied more in the outdoor bioreactors.

Microbial Population Differences and Dominant ASVs

To study the bacterial population composition trends at a more granular level, a principal coordinate analysis plot of Bray–Curtis differences between sample ASV compositions was produced (Fig. 6). The only grouping of samples according to the indoor or outdoor BRs or seasons is the cluster of orange points on the left-hand side representing the indoor bioreactors from spring 2020 to fall 2020. During this period, the microbial population composition of these two BRs appeared to be stable. The same observation was not applicable for the other BRs.

To better understand the potential functional characteristics of the BR bacteria populations, the prevalence of dominant ASVs (> 1% of the total population) was studied (Fig. 7). *Geobacter*, an iron-reducing genus (Lovley et al. 2011), was the most dominant Desulfobacterota and was prevalent in the indoor BRs in the fall of 2019. Only one ASV was classified as a known sulfate-reducing bacteria genus, *Desulfovulbus*. It appeared to be consistently dominant in all BRs. The other Desulfobacterota were *Citrifermentans* and MSBL7. The former, also known as *Geomonas*, has one member that is a Fe-reducing species (Xu et al. 2019). MSBL7 is an uncharacterized environmental

group. The most dominant Firmicutes ASVs were classified in an uncharacterized environmental group R-7 in the family Christensenellaceae, a known genus member that are obligately anaerobic fermenters producing acetate and other organic acids from sugars (Morotomi et al. 2012).

Sugar-fermenting microorganisms were a major part of the bacterial communities in all BRs, as another dominant Firmicutes ASV was classified as *Saccharofermentans* (Chen et al. 2010). Of the Bacteroidota, the ASV classified as Bacteroidetes_vadinHA17 is thought to be a species adapted to the degradation of recalcitrant organic matter (Mei et al. 2020a). Finally, the other important phylum, Proteobacteria, contained three functionally versatile dominant ASVs associated with nutrient cycling and phototrophy.

Overall, the diversity of ASVs was constrained, with the number of ASVs in each sample ranging from 100 to 350 (supplemental Table S-2), which is within the range typical for MIW BRs but far less than the number of dominant ASVs in soils or vegetated wetlands, for example. The bubble plot of dominant ASVs in Fig. 7 is not very sparse, indicating that many ASVs were found in all of the BRs most of the time. The dominant ASVs were common among the BR populations, with differences being mostly due to compositional variation. The only exception was the Proteobacteria *Stenotrophomonas* ASV in BR2a_09/20. There are eight members of this genus,

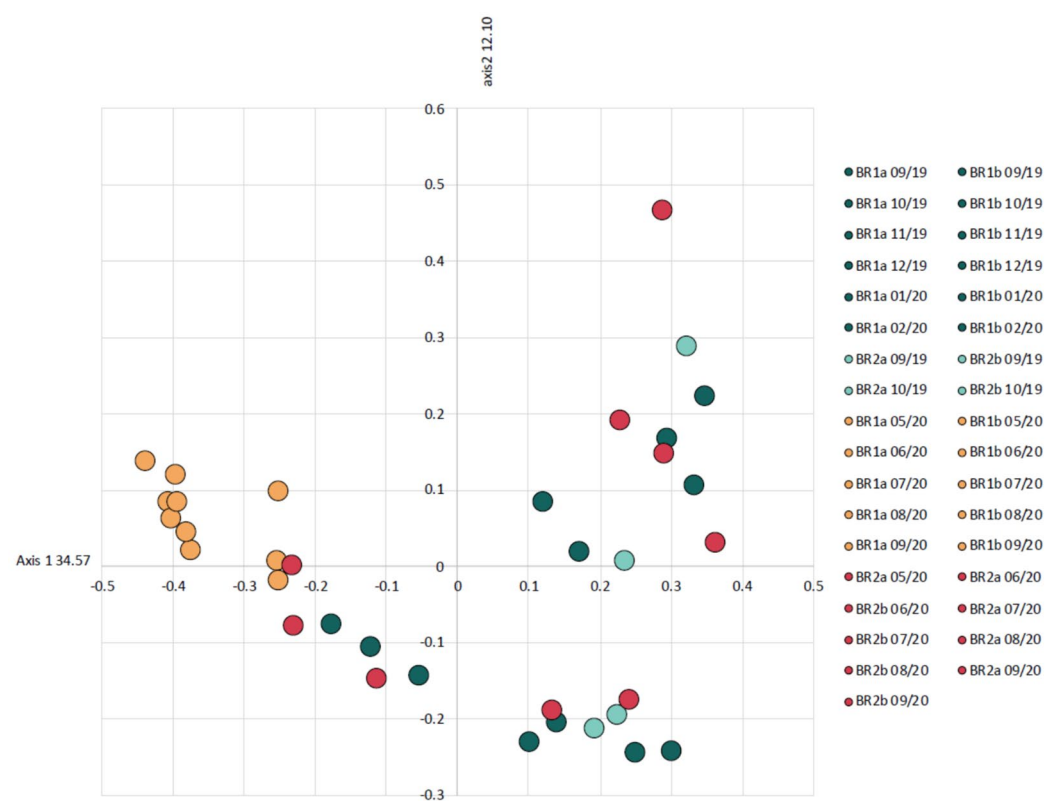
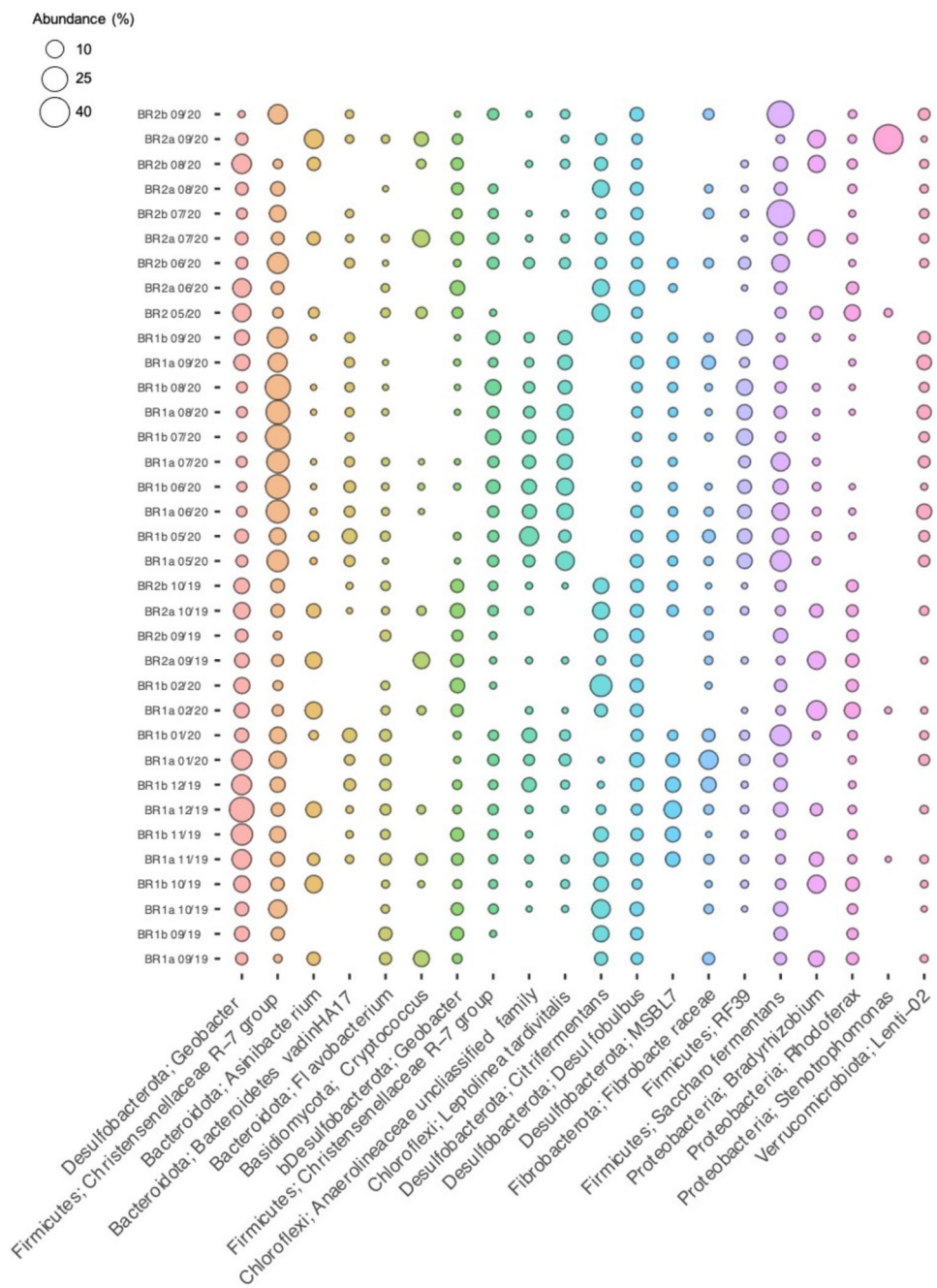


Fig. 6 Principal coordinate analysis based on the differences (Bray–Curtis) between samples in their ASV compositions. Samples from Fall 2019/Winter 2020 are dark (BR1) and light (BR2) blue-green, and samples from Spring 2020 onwards are orange (BR1) to red (BR2)

Fig. 7 Dominant ASVs (> 1% of the population in each bioreactor) in the bioreactors over time



at the time of writing, some of which are known to be tolerant to high concentrations of metals and are important for N and S cycling (Ryan et al. 2009).

Discussion

Tracking of Bacterial Activity and Performance of the BRs

Throughout the experiment, the MIW fed into the BRs had a circumneutral to slightly alkaline pH, indicating neutral

mine drainage conditions. EC, Ca, metal(lloid), TOC, and sulfate concentrations in the MIW were lowest in fall 2019, increased in winter 2019–2020, and then decreased during the 2020 freshet. This trend in water chemistry is typical of seasonal variation: after the thawing period in late spring and throughout summer and early fall, the surface watershed in the Yukon is ice-free, and water flows freely, lowering EC and concentrations in MIW due to dilution (Nielsen et al. 2018a). When the temperatures were below freezing, as they are during winter, the volume of free water available on the surface is reduced, and thus, MIW is more concentrated in

dissolved solids, explaining the observed increases in EC, Ca, metal(loid)s, and sulfate concentrations.

The Ca concentrations and EC measured in the BR effluents were at the same levels as those in the MIW feed when considering an offset of 11 days, which was the retention time of the MIW in the BRs. The pH also remained consistent between the MIW feed and BR effluents. Thus, it was concluded that: (i) none of the Ca precipitated as sulfate minerals, such as gypsum or ettringite, in the BRs, and (ii) water chemistry parameters such as pH, Ca concentrations, and EC were not strongly modified by the BRs.

Sulfate concentrations in the BR1s and BR2s effluents were lower than those in the MIW feed most of the time ($\approx 90\%$ for the four BRs), indicating that sulfate was being reduced in all of the BRs. Negative sulfate removal occurred only rarely (two occasions in BR1a, one occasion in BR1b and BR2a) when the sulfate concentration in the MIW was low. The presence of SRB bacteria in the genus *Desulfobulbus*, which were observed in all BRs, supports the hypothesis that sulfate removal was occurring through biological reduction, with sulfate acting as an electron acceptor and molasses-derived carbon compounds as electron donors (Muyzer and Stams 2008). In addition, optimal ORP values for SRB to reduce sulfate to sulfide that are in the range of -100 to -300 mV (Gibert et al. 2002), were measured in the BRs. In BR1a and BR1b, sulfate removal percentage appeared to correlate with temperature, with lower reduction observed during winter. This was expected since most SRB species are mesophiles, meaning that the optimal temperatures for their growth and activity are between 25 and 35 °C, and similar temperature dependent observations were made in a previous BR study (Nielsen et al. 2018a). Sulfate reduction percentages varied importantly during the thaw period between the four BRs (-60% in BR1a to 95% in BR2b), and between the duplicate BRs located inside or outside. From June until the end of the study, sulfate reduction in all BRs was maintained over 80%. These results indicate that the thaw period impacted strongly the BRs, but in an unpredictable way. However, they also indicate that SRB re-established their bacterial activity quickly after thaw in the outdoor BRs with only a small delay between the increase in temperature and the increase in bacterial activity. Since the SRB related ASVs present before and after winter were taxonomically similar, the SRB active from spring 2020 onwards could have been those that survived freeze/thaw inside BR2s. It is unknown what microorganisms were present in the MIW or how consistent this was before and after winter. If different microbial species entered the BRs with the spring freshet MIW, they did not change the taxonomy of the SRB population.

Another tracker of bacterial activity in the BRs was carbon removal, which was expected due to consumption by

active bacteria. The presence of bacteria involved in the decomposition of organic C compounds, and other bacteria (SRB and iron-reducing bacteria) that are heterotrophic, suggests that carbon source consumption must be taking place. However, for the first four months of the experiment, carbon was released rather than removed in BR1s. Leaching experiments using the same spruce wood chips as were used in the BRs revealed that up to 6.5 mg-C/g woodchips (dry weight) were leached over five weeks. Based on these results, it is likely that soluble carbon compounds were being released from the spruce wood chips in the BRs, at least during the initial period after start-up. During this period, the amount of carbon released was sporadically greater than the carbon consumed by bacterial activity. Presence of microbial taxa associated with degradation of recalcitrant organic material, such as hard to breakdown lignocellulosic compounds (i.e. Bacteroidetes_vadinHA17; Mei et al. 2020b), provides evidence for the biological decomposition of the wood chips in the BRs. After four months, the percentage of carbon removal in BR1s became positive, but the values continued to alternate between positive and negative for BR2s until the end of the experiment. A likely explanation for this was that biodegradation of wood chips occurred to a greater extent in the indoor BRs since they operated over the entire experimental period, whereas freezing of the outdoor BRs prevented any bacterial activity for enzymatic hydrolysis of cellulosic material in the woodchips during winter. Heterotrophic bacteria such as the Firmicutes *Saccharofermentas* were dominant throughout all of the BRs and seasons but were present at higher relative abundances in BR2 than BR1 in the summer and fall of 2020. Members of this genus were likely growing on the sugars still being produced in BR2 from enzymatic hydrolysis of the woodchips. Decomposition of wood chips inside the BRs might be beneficial since this would increase the supply of carbon for bacterial growth. However, this supply will diminish over time as all the degradable C is depleted, which seemed to be the case for BR1. Thus, extraneous carbon addition in the form of cost-effective natural sources such as molasses will be needed for long term reliable performance of BRs.

Impact of Bacterial Activity on Metal(loid)s Removal

The Sb concentrations in the MIW did not vary seasonally and was marked by two spike events (Fig. 3a). The Se levels in MIW seemed to be more affected by seasonal variations, with the highest concentration in summer (Fig. 4a). No strong correlations ($R \leq 0.9$) were detected between Sb or Se and major elements such as sulfate, carbon, Fe, Ca, or other metals (Pb, Cu, Cd, Pb) in the MIW. After one month of operation, in October 2019, the BRs started

to remove Sb and Se, coinciding with signs of sulfate reduction.

Sb likely entered the BRs as Sb(V) since the MIW used in this study was collected at the surface (Johnston et al. 2020). Processes that might be involved in Sb removal in the reducing environment of the BRs include microbial Sb(V) reduction to Sb(III), microbial methylation, and abiotic Sb(V) reduction by S(-II) and/or Fe(-II) (Zhang et al. 2022). Microbial Sb(V) reduction can take place through respiratory and non-respiratory metabolic pathways. For instance, Sb(V) can be enzymatically reduced by SRB for energy (Wang et al. 2013), with the reduced Sb immobilized via antimony sulfide formation (Liu et al. 2022). Other types of bacteria have been reported to mediate immobilization and remove Sb, under both aerobic and anaerobic conditions, including those that oxidize the more toxic Sb(III) to the less toxic Sb(V) (Deng et al. 2021). None of the Sb resistant genera reported in the Deng et al. 2021 study were among those identified in the BRs. Biological Sb methylation can occur under anoxic conditions as a detoxification mechanism and has been observed in various environments, but the molecular mechanism remains poorly understood, and only a few bacterial species with this capability have been identified so far (Liu et al. 2022). None of the latter genera reported in Liu et al. 2022 were identified in the BRs. Another path to Sb(V) removal is through SRB species (Wang et al. 2013). Of all the possible Sb biotic removal mechanisms, we hypothesize that biotic removal mediated by SRB was very likely occurring in the BRs due to the prevalence of *Desulfovibrio* species. The presence of Fe-reducing bacteria in the BRs, the reducing conditions in the BRs (Jia et al. 2022), and the higher concentrations of Fe compared to Sb (mg/L vs. $\mu\text{g}/\text{L}$) suggested that Sb-Fe oxide precipitation could occur in the BRs, despite the continuous release of Fe in the effluents. Abiotic precipitation of antimony sulfide was another possible Sb removal mechanism, given the presence of sulfide (HS^- , S^{2-}) coming from sulfate reduction (Ramírez-Patiño et al. 2023).

Overall, both the indoor and outdoor BRs were successful at removing Se from the MIW. The removal percentage was between 0.5 and 94% for BR1s and 44 and 95% for BR2s. Post-winter, during the thaw period (May 2020), BR2s recommenced removing Se, though at lower percentages (60 and 78% for BR1a and BR1b, respectively) than in BR1s (87 and 92% for BR1a and BR1b, respectively) during the same period. By summer 2020, both BR1s and BR2s removed similar amounts of Se. These results indicate that while BR2's Se removal capacity was impacted by freezing, the BR recovered quickly, achieving the same removal capacity as BR1 after only a month.

Se speciation was not performed, and so it is not known which chemical forms were present in the MIW or in the BR

effluents. As the MIW was sourced at the surface where conditions were oxidizing, then Se may be present as selenate (SeVI , SeO_4^{2-}) or selenite (SeIV , SeO_3^{2-}), depending on the pH and redox conditions (Yan et al. 2022). Many bacteria can reduce selenate as an electron acceptor for energy and growth. These include those with selenate specific reductases, such as *Thauera selenatis* (Macy et al. 1993), or denitrifying bacteria with nitrate reductases that are versatile (e.g. *Paracoccus* sp.) (Sabaty et al. 2001). Selenate or selenite reduction can occur aerobically or anaerobically (Avendaño et al. 2016). None of the species that have been characterized at the time of publishing as Se-reducing bacteria were among the dominant AVS genera identified in the BR metagenomes. However, Se removal has been observed in SRB bioreactors mediated through SRB activity (Hockin and Gadd 2006). Due to the presence of SRB in the BRs, the latter was a probable mechanism. Selenate is the most soluble and mobile form of Se. When selenate is reduced to selenite, then this chemical form has a higher affinity for adsorption than selenate. If selenite reduction to selenite was occurring in the BRs, then Se removal might have occurred through selenite binding to solids such as Fe oxy(hydrox)ides (Balistrieri and Chao 1990).

The relative abundance of the microbial ASVs in the BR1s were more stable across time points after the Spring 2020 thaw than in BR2s. The greater relative abundance variability observed in BR2s vs. BR1s during this period is attributed to the effects of freeze–thaw in BR2. Nevertheless, many of the same dominant genera were present both before and after the freeze–thaw, suggesting that biological removal mechanisms for Se and Sb were consistent across seasons. Since the microbial population included phylotypes with assumed phenotypes with metabolic potential for C, sulfate, Se and Sb removal, and Fe release, the successful performance of all the BRs was not limited by a functionally essential microbial community. The presence of this microbial community might have contributed to the relatively quick re-establishment of BR2's performance post thaw. Indeed, other studies also have observed that distribution of key metabolic functions across different genera coexisting in BRs favors process stability (Ayala-Muñoz et al. 2021). Overall, this study demonstrated that the freezing of BRs did not substantially affect their ability to remove sulfate, Se, and Sb from MIW.

Conclusions

The present study provides evidence that BRs inoculated with locally sourced bacterial populations maintain their capability to remove sulfate, as well as Sb and Se metal(lloid)s despite being subject to a seasonal freeze–thaw cycle. BRs

that were located inside a heated shed, maintained at $\geq 5^{\circ}\text{C}$, successfully removed Se and Sb most of the year. The indoor and outdoor BRs removed up to 95% of the Se and Sb. It's important to note that on a few occasions, the removal efficiency of Se and Sb were negative, specifically at the beginning of the BRs operation, when the temperature changed, and in the event of low concentrations in the MIW. The BRs that were located outdoors removed similar amounts of Se and Sb as the BRs inside the shed prior to freezing. After the spring thaw, removal percentages of Se and Sb in the outdoor BRs were slightly lower than those achieved in BR1s. However, after thawing and during the subsequent summer and fall, Se and Sb removal was similar in both indoor and outdoor bioreactors.

Microbial population composition analysis indicated that the taxonomic groups aligned with the expected biological metal(loid)s removal mechanisms were present. These included bacteria involved in iron reduction, sulfate reduction, and decomposition of organic material. Based on the presence of *Desulfobulbus* genera and previous studies, the most likely postulated mechanism for Se and Sb removal was mediation by SRB, either directly through dissimilatory reduction or indirectly through sulfide precipitation. The freeze–thaw events over winter and spring did not disrupt the microbial population composition with similar dominant bacteria being present before and after. Using inoculum sourced directly on site might explain these interesting and positive observations: The bacterial consortium growing inside the BRs contains bacteria naturally present in the (sub)arctic region and, thus, adapted to freezing events occurring during winter. One pitfall of using anaerobic BRs for MIW treatment is the release of Fe in BRs' effluents. Fe, like other chemical elements, is a regulated parameter in the mining industry, and its release in the environment following water treatment needs to be considered when designing future semi-passive water treatment systems. Further studies focusing on several freeze–thaw cycles, various inoculums, and different contaminants would allow us to extend and validate the promising results obtained in this study.

Supplementary Information The online version contains supplementary material available at <https://doi.org/10.1007/s10230-024-00999-x>.

Acknowledgements The Natural Sciences and Engineering Research Council of Canada (NSERC) is acknowledged for supporting this work through the Industrial Research Chair in Northern Mine Remediation at Yukon University. The Victoria Gold Staff are acknowledged for supporting the fieldwork. This pilot scale experiment would not have been possible without weekly monitoring and maintenance that was performed by the Victoria Gold environmental team (related industrial report: Nielsen et al. 2023 et al. 2023). The authors also thank the two anonymous reviewers for their comments and support in improving the quality of this article.

Data availability Data will be available upon demand to the corresponding author.

Open Access This article is licensed under a Creative Commons Attribution 4.0 International License, which permits use, sharing, adaptation, distribution and reproduction in any medium or format, as long as you give appropriate credit to the original author(s) and the source, provide a link to the Creative Commons licence, and indicate if changes were made. The images or other third party material in this article are included in the article's Creative Commons licence, unless indicated otherwise in a credit line to the material. If material is not included in the article's Creative Commons licence and your intended use is not permitted by statutory regulation or exceeds the permitted use, you will need to obtain permission directly from the copyright holder. To view a copy of this licence, visit <http://creativecommons.org/licenses/by/4.0/>.

References

Allison SD, Martiny JBH (2008) Resistance, resilience, and redundancy in microbial communities. *Proc Natl Acad Sci USA* 105:11512–11519

Avendaño R, Chaves N, Fuentes P, Sánchez E, Jiménez JI, Chavarría M (2016) Production of selenium nanoparticles in *Pseudomonas putida* KT2440. *Sci Rep* 6:37155

Ayala-Muñoz D, Simister RL, Crowe SA, Macalady JL, Burgos WD (2021) Functional redundancy imparts process stability to acidic Fe (II)-oxidizing microbial reactors. *Environ Microbiol* 23:3682–3694

Baldwin SA, Mattes A, Rezadeh-bashi M, Taylor J (2016) Seasonal microbial population shifts in a bioremediation system treating metal and sulfate-rich seepage. *Minerals* 6:36

Balistreri LS, Chao TT (1990) Adsorption of selenium by amorphous iron oxyhydroxide and manganese dioxide. *Geochim Cosmochim Acta* 54:739–751

Ben Ali HE, Neculita CM, Molson JW, Maqsoud A, Zagury GJ (2019) Performance of passive systems for mine drainage treatment at low temperature and high salinity: a review. *Miner Eng* 134:325–344

Ben Ali HE, Neculita CM, Molson JW, Maqsoud A, Zagury GJ (2020) Salinity and low temperature effects on the performance of column biochemical reactors for the treatment of acidic and neutral mine drainage. *Chemosphere* 243:125303

Bolyen E, Rideout JR, Dillon MR, Bokulich NA, Abnet CC, Al-Ghalith GA, Alexander H, Alm EJ, Arumugam M, Asnicar F (2019) Reproducible, interactive, scalable and extensible microbiome data science using QIIME 2. *Nat Biotechnol* 37:852–857

Brodie Consulting Ltd., Casino Mining Corporation (2013) Casino Mine Closure Plan [WWW Document]. Casino Mining Corporation: Casino Project Conceptual Closure and Reclamation Plan. https://emrlibrary.gov.yk.ca/minerals/MajorMines/casino/proposal_2014_0002_appendices/04A_conceptual_closure_and_reclamation_plan.pdf. Accessed 3.12.24.

Callahan BJ, McMurdie PJ, Rosen MJ, Han AW, Johnson AJA Holmes SP (2016) DADA2: High-resolution sample inference from Illumina amplicon data. *Nat Methods* 13: 581–583

Chen S, Niu L, Zhang Y (2010) *Saccharofermentans acetigenes* gen. nov., sp. nov., an anaerobic bacterium isolated from sludge treating brewery wastewater. *Int J Syst Evol Microbiol* 60:2735–2738

Clyde EJ, Champagne P, Jamieson HE, Gorman C, Sourial J (2016) The use of a passive treatment system for the mitigation of acid mine drainage at the Williams Brothers Mine (California): pilot-scale study. *J Clean Prod* 130:116–125

Deng R, Chen Y, Deng X, Huang Z, Zhou S, Ren B, Jin G, Hursthouse A (2021) A critical review of resistance and oxidation mechanisms of Sb-oxidizing bacteria for the bioremediation of Sb (III) pollution. *Front Microbiol* 12:738596

Doyle MO, Otte ML (1997) Organism-induced accumulation of iron, zinc and arsenic in wetland soils. *Environ Pollut* 96:1–11

El Kilani MA, Jouini M, Rakotonimaro TV, Neculita CM, Molson JW, Courcelles B, Dufour G (2021) In-situ pilot-scale passive biochemical reactors for Ni removal from saline mine drainage under subarctic climate conditions. *J Water Proc Eng* 41:102062

Gallagher N, Blumenstein E, Rutkowski T, DeAngelis J, Reisman D, Progess C (2012) Passive treatment of mining influenced wastewater with biochemical reactor treatment at the standard mine Superfund site, Crested butte, Colorado. *Proc, America Soc of Mining and Reclamation*, pp 137–153

Genty T, Bussière B, Benzaazoua M, Neculita CM, Zagury GJ (2018) Changes in efficiency and hydraulic parameters during the passive treatment of ferriferous acid mine drainage in biochemical reactors. *Mine Water Environ* 37:686–695

Gibert O, de Pablo J, Cortina JL, Ayora C (2002) Treatment of acid mine drainage by sulphate-reducing bacteria using permeable reactive barriers: a review from laboratory to full-scale experiments. *Rev Environ Sci Biotechnol* 1:327–333

Habe H, Sato Y, Aoyagi T, Inaba T, Hori T, Hamai T, Hayashi K, Kobayashi M, Sakata T, Sato N (2020) Design, application, and microbiome of sulfate-reducing bioreactors for treatment of mining-influenced water. *Appl Microbiol Biotechnol* 104:6893–6903

Haley S, Klick M, Szymoniak N, Crow A (2011) Observing trends and assessing data for Arctic mining. *Polar Geogr* 34:37–61

Harrington J, Harrington J, Lancaster E, Gault A, Woloshyn K (2015) Bioreactor and in situ mine pool treatment options for cold climate mine closure at Keno Hill, YT. Agreeing on solutions for more sustainable mine water management. *Gecamin, Santiago/Chile*, pp 1–10

Health Canada/Santé Canada (2024) Guidelines for Canadian Drinking Water Quality: Guideline Technical Document – Antimony [WWW Document]. <https://www.canada.ca/content/dam/hc-sc/images/services/publications/healthy-living/guidelines-canadian-drinking-water-quality-guideline-technical-document-antimony/drinking-water-quality-guidelines-antimony-en-web-27-23-3557.pdf> (accessed 3.13.24).

Hockin S, Gadd GM (2006) Removal of selenate from sulfate-containing media by sulfate-reducing bacterial biofilms. *Environ Microbiol* 8:816–826

Jia X, Ma L, Liu J, Liu P, Yu L, Zhou J, Li W, Zhou W, Dong Z (2022) Reduction of antimony mobility from Sb-rich smelting slag by *Shewanella oneidensis*: integrated biosorption and precipitation. *J Hazard Mater* 426:127385

Johnson DB, Hallberg KB (2005) Acid mine drainage remediation options: a review. *Sci Total Environ* 338:3–14

Johnson H, Cho H, Choudhary M (2019) Bacterial heavy metal resistance genes and bioremediation potential. *Comput Mol Biosci* 9(1):1–12. <https://doi.org/10.4236/cmb.2019.91001>

Johnston SG, Bennett WW, Doriean N, Hockmann K, Karimian N, Burton ED (2020) Antimony and arsenic speciation, redox-cycling and contrasting mobility in a mining-impacted river system. *Sci Total Environ* 710:136354

Laroche E, Joulian C, Duee C, Casiot C, Héry M, Battaglia-Brunet F (2023) Bio-precipitation of arsenic and antimony in a sulfate-reducing bioreactor treating real acid mine drainage water. *FEMS Microbiol Ecol* 99, fiad075. <https://doi.org/10.1093/femsec/fiad075>

Leppänen JJ, Weckström J, Korhola A (2017) Multiple mining impacts induce widespread changes in ecosystem dynamics in a boreal lake. *Sci Rep* 7:10581

Liu H, Sun W, Häggblom MM (2022) Microbial transformations of antimony. Springer, *Microbial Metabolism of Metals and Metalloids*, pp 223–254

Liu L, Wang S, Guo X, Zhao T, Zhang B (2018) Succession and diversity of microorganisms and their association with physicochemical properties during green waste thermophilic composting. *Waste Manage* 73:101–112

Lovley DR, Ueki T, Zhang T, Malvankar NS, Shrestha PM, Flanagan KA, Aklujkar M, Butler JE, Giloteaux L, Rotaru AE (2011) Geobacter: the microbe electric's physiology, ecology, and practical applications. *Adv Microb Physiol* 59:1–100

Lum JE, Schoepfer VA, Jamieson HE, McBeth JM, Radková AB, Walls MP, Lindsay MBJ (2023) Arsenic and antimony geochemistry of historical roaster waste from the Giant Mine, Yellowknife. *Canada J Hazard Mater* 458:132037

Luo Q, Tsukamoto TK, Zamzow KL, Miller GC (2008) Arsenic, selenium, and sulfate removal using an ethanol-enhanced sulfate-reducing bioreactor. *Mine Water Environ* 27:100–108

Macy JM, Rech S, Auling G, Dorsch M, Stackebrandt E, Sly LI (1993) *Thauera selenatis* gen. nov., sp. nov., a member of the beta subclass of Proteobacteria with a novel type of anaerobic respiration. *Int J Syst Evol Microbiol* 43:135–142

Martin AJ, Jones R, Buckwalter-Davis M (2009) Passive and semi-passive treatment alternatives for the bioremediation of selenium from mine waters

Mei R, Nobu MK, Narihiro T, Liu WT (2020) Metagenomic and metatranscriptomic analyses revealed uncultured bacteroidales populations as the dominant proteolytic amino acid degraders in anaerobic digesters. *Front Microbiol* 11:593006

Morotomi M, Nagai F, Watanabe Y (2012) Description of *Christensenella minuta* gen. nov., sp. nov., isolated from human faeces, which forms a distinct branch in the order Clostridiales, and proposal of Christensenellaceae fam. nov. *Int J Syst Evol Microbiol* 62:144–149

Muyzer G, Stams AJM (2008) The ecology and biotechnology of sulphate-reducing bacteria. *Nat Rev Microbiol* 6:441–454

Neculita C, Zagury GJ, Bussière B (2007) Passive treatment of acid mine drainage in bioreactors using sulfate-reducing bacteria: Critical review and research needs. *J Environ Qual* 36:1–16

Ness I, Janin A, Stewart K (2014) Passive treatment of mine impacted water in cold climates: a review. *Yukon Research Centre, Yukon College*

Nielsen G, Hatam I, Abuan KA, Janin A, Coudert L, Blais JF, Mercier G, Baldwin SA (2018a) Semi-passive in-situ pilot scale bioreactor successfully removed sulfate and metals from mine impacted water under subarctic climatic conditions. *Water Res* 140:268–279

Nielsen G, Janin A, Coudert L, Blais JF, Mercier G (2018b) Performance of sulfate-reducing passive bioreactors for the removal of Cd and Zn from mine drainage in a cold climate. *Mine Water Environ* 37:42–55

Nielsen G, McGrath B, Gilmar M, Zurkan C, Janzen I, Moore R, Kaur I, Desmau M (2023) Pilot scale Bioreactors at Eagle Gold Mine site: Studying bacterial populations' adaptation to seasonal freeze and thaw cycles and their capacity to remove Sb, Se and As. Whitehorse. www.yukon.ca/sites/default/files/inline-files/Pilot ScaleBREagleGoldMine_3Year_Aug2023_2.pdf

Odom JM, Singleton R (1993) The Sulfate-Reducing Bacteria: Contemporary Perspectives. Springer

Parada AE, Needham DM, Fuhrman JA (2016) Every base matters: assessing small subunit rRNA primers for marine microbiomes with mock communities, time series and global field samples. *Environ Microbiol* 18:1403–1414

Price PB, Sowers T (2004) Temperature dependence of metabolic rates for microbial growth, maintenance, and survival. *Proc Natl Acad Sci USA* 101:4631–4636

Ramírez-Patiño J, Pérez-Trevilla J, Cervantes FJ, Moreno-Andrade I (2023) Removal of antimony by dissimilatory and sulfate-reducing pathways in anaerobic packed bed bioreactors. *J Chem Technol Biotechnol* 98:932–939

Reisman D, Rutkowski T, Smart P, Gusek J, Sieczkowski M (2009) Passive treatment and monitoring at the standard mine superfund site Crested Butte, CO. *Proc, America Soc of Mining and Reclamation*, pp 1107–1128

Robador A, Brüchert V, Jørgensen BB (2009) The impact of temperature change on the activity and community composition of sulfate-reducing bacteria in arctic versus temperate marine sediments. *Environ Microbiol* 11:1692–1703

Rutkowski T (2013) Passive treatment of mining influenced wastewater at the standard mine superfund site, Crested Butte, Colorado, USA. *Proc, Mine Water Solutions Conf*, pp. 15–17

Ryan RP, Monchy S, Cardinale M, Taghavi S, Crossman L, Avison MB, Berg G, Van Der Lelie D, Dow JM (2009) The versatility and adaptation of bacteria from the genus *Stenotrophomonas*. *Nat Rev Microbiol* 7:514–525

Sabat M, Avazeri C, Pignol D, Vermeglio A (2001) Characterization of the reduction of selenate and tellurite by nitrate reductases. *Appl Environ Microbiol* 67:5122–5126

Sánchez-Andrea I, Sanz JL, Bijnmans MFM, Stams AJM (2014) Sulfate reduction at low pH to remediate acid mine drainage. *J Hazard Mater* 269:98–109

Sengupta M (2021) Environmental Impacts of Mining: Monitoring. CRC Press, Restoration and Control

Sharmin F, Wakelin S, Huygens F, Hargreaves M (2013) Firmicutes dominate the bacterial taxa within sugar-cane processing plants. *Sci Rep* 3:3107

Sinharoy A, Lens PNL (2020) Biological removal of selenate and selenite from wastewater: options for selenium recovery as nanoparticles. *Curr Pollut Rep* 6:230–249

Tiainen H, Sairinen R, Sidorenko O (2015) Governance of Sustainable Mining in Arctic Countries: Finland, Sweden, Greenland & Russia. *Arctic Yearbook* 2015:132

Victoria Gold Corp (2022) Eagle Gold Mine Closure Plan [WWW Document]. Eagle Gold Mine Reclamation And Closure Plan. URL <https://emr-ftp.gov.yk.ca/emrweb/COMM/major-mines/eagle-gold/emr-mm1-eg-reclamation-closure-plan-version-2022-01.pdf> (accessed 3.12.24)

Walters W, Hyde ER, Berg-Lyons D, Ackermann G, Humphrey G, Parada A, Gilbert JA, Jansson JK, Caporaso JG, Fuhrman JA (2016) Improved bacterial 16S rRNA gene (V4 and V4–5) and fungal internal transcribed spacer marker gene primers for microbial community surveys. *mSystems* 1, e00009–15

Wang H, Chen F, Mu S, Zhang D, Pan X, Lee DJ, Chang JS (2013) Removal of antimony (Sb(V)) from Sb mine drainage: Biological sulfate reduction and sulfide oxidation–precipitation. *Bioresour Technol* 146:799–802. <https://doi.org/10.1016/j.biortech.2013.08.002>

Warnow T (2015) Encyclopedia of Metagenomics, Springer, Boston, MA. <https://doi.org/10.1007/978-1-4899-7478-5>

Wright IA, McCarthy B, Belmer N, Price P (2015) Subsidence from an underground coal mine and mine wastewater discharge causing water pollution and degradation of aquatic ecosystems. *Water Air Soil Pollut* 226:1–14

Xu Z, Masuda Y, Itoh H, Ushijima N, Shiratori Y, Senoo K (2019) *Geomonas oryzae* gen. nov., sp. nov., *Geomonas edaphica* sp. nov., *Geomonas ferrireducens* sp. nov., *Geomonas terrae* sp. nov., four ferric-reducing bacteria isolated from paddy soil, and reclassification of three species of the genus *Geobacter* as members of the genus *Geomonas* gen. nov. *Front Microbiol* 10: 2201

Yan S, Cheng KY, Ginige MP, Morris C, Deng X, Li J, Song S, Zheng G, Zhou L, Kaksonen AH (2022) Sequential removal of selenate, nitrate and sulfate and recovery of elemental selenium in a multi-stage bioreactor process with redox potential feedback control. *J Hazard Mater* 424:127539

Younger PL, Banwart SA, Hedin RS, Younger PL, Banwart SA, Hedin R (2002) Mine Water Hydrology. Springer

Zaluski MH, Trudnowski JM, Harrington-Baker MA, Bless DR (2003) Post-mortem findings on the performance of engineered SRB field-bioreactors for acid mine drainage control. *Proc, ICARD 2003: Sixth International Conf on Acid Rock Drainage* 303043: 845–854. DOI.org/<https://doi.org/10.7939/r3-nezs-r530>

Zhang Y, O'Loughlin EJ, Kwon MJ (2022) Antimony redox processes in the environment: a critical review of associated oxidants and reductants. *J Hazard Mater* 128607

Zhao YG, Wang AJ, Ren NQ (2010) Effect of carbon sources on sulfidogenic bacterial communities during the starting-up of acidogenic sulfate-reducing bioreactors. *Bioresour Technol* 101:2952–2959